About the Author

Dr. Tasić-Otasevic is a professor in the Department of Microbiology and Immunology, University of Niš, and Department of Microbiology and Parasitology, Public Health Institute. Her research interests are clinical and diagnostic microbiology, skin and genital infections, antimicrobial resistance, fungal pathogens, vectorborne zoonosis, and health promotion.

References

1. Genchi C, Kramer LH. The prevalence of *Dirofilaria immitis* and *D. repens* in the Old World. Vet Parasitol. 2020;280:108995. https://doi.org/10.1016/j.vetpar.2019.108995
2. Gabrielli S, Mangano V, Furzi F, Oliva A, Vita S, Poscia R, et al. Molecular identification of new cases of human dirofilariosis (*Dirofilaria repens*) in Italy. Pathogens. 2021;10:251. https://doi.org/10.3390/pathogens10020251
3. Simón F, Diosdado A, Siles-Lucas M, Kartashev V, González-Miguel J. Human dirofilariosis in the 21st century: a scoping review of clinical cases reported in the literature. Transbound Emerg Dis. 2022;69:2424–39. https://doi.org/10.1111/tbed.14210
4. Pupić-Bakrač A, Pupić-Bakrač J, Beck A, Jurković D, Polkinghorne A, Beck R. *Dirofilaria repens* microfilaremia in humans: case description and literature review. One Health. 2021;13:100306. https://doi.org/10.1016/j.onehlt.2021.100306
5. Tamura K, Stecher G, Kumar S. MEGA11: molecular evolutionary genetics analysis version 11. Mol Biol Evol. 2021;38:3022–7. https://doi.org/10.1093/molbev/msab120
6. Ciuca L, Simòn F, Rinaldi L, Kramer L, Genchi M, Cringoli G, et al. Seroepidemiological survey of human exposure to *Dirofilaria* spp. in Romania and Moldova. Acta Trop. 2018;187:169–74. https://doi.org/10.1016/j.actatropica.2018.07.012
7. Savić S, Stosic MZ, Marcic D, Hernández I, Potkonjak A, Otasevic S, et al. Seroepidemiological study of canine and human dirofilariasis in the endemic region of northern Serbia. Front Vet Sci. 2020;7:571. https://doi.org/10.3389/fvets.2020.00571
8. Otranto D, Eberhard ML. Zoonotic helminths affecting the human eye. Parasit Vectors. 2011;4:41. https://doi.org/10.1186/1756-3305-4-41
9. Simón F, Siles-Lucas M, Morchón R, González-Miguel J, Mellado I, Carretón E, et al. Human and animal dirofilariasis: the emergence of a zoonotic mosaic. Clin Microbiol Rev. 2012;25:507–44. https://doi.org/10.1128/CMR.00012-12
10. Tasić-Otašević S, Savić S, Jurhar-Pavlova M, Stefanovska J, Stalević M, Ignjatović A, et al. Molecular survey of *Dirofilaria* and *Leishmania* species in dogs from central Balkan. Animals (Basel). 2022;12:911. https://doi.org/10.3390/ani12070911

Address for correspondence: Simona Gabrielli, Department of Public Health and Infectious Diseases, Sapienza University of Rome, Piazzale Aldo Moro 5, Rome 00185, Italy; email: simona.gabrielli@uniroma1.it

Anthropogenic Transmission of SARS-CoV-2 from Humans to Lions, Singapore, 2021

Yin Cheong Aden Ip, Adrian Tan, Jasmine Ong, Charlene Judith Fernandez, Clara Lau, Wai Kwan Wong, Siow Foong Chang, Him Hoo Yap, Kenneth B.H. Er

Author affiliation: National Parks Board, Singapore

DOI: https://doi.org/10.3201/eid2912.221916

In Singapore, 10 captive lions tested positive for SARS-CoV-2 by real-time PCR. Genomic analyses of nanopore sequencing confirmed human-to-animal transmission of the SARS-CoV-2 Delta variant. Viral genomes from the lions and zookeeper shared a unique spike protein substitution, S:A1016V. Widespread SARS-CoV-2 transmission among humans can increase the likelihood of anthroponosis.

We investigated natural SARS-CoV-2 infection in captive African (*Panthera leo*) and Asiatic (*Panthera leo persica*) lions at a zoo in Singapore during increased Delta variant community infections. Understanding virus dynamics in different hosts is crucial for preventing interspecies transmission and protecting endangered species (*1*,*2*).

We studied 14 lions, 9 Asiatic and 5 African, that were housed in separate enclosures. On November 6, 2021, respiratory signs developed in a male Asiatic lion (AS-M1) (Appendix 1, https://wwwnc.cdc.gov/EID/article/29/12/22-1916-App1.pdf). On November 7, three Asiatic lionesses (AS-F1, AS-F2, and AS-F3) in the same enclosure exhibited similar clinical signs. A male African lion (AF-M3) in a separate enclosure developed clinical signs on November 8.

Eighteen zookeepers cared for and had close (within ≈1 m) but not direct contact with the lions. Six zookeepers tested COVID-19–positive beginning November 1, 2021, and 4 experienced mild respiratory symptoms starting on November 2.

To minimize stress on the animals, only 2 lions that had more severe signs, AS-M1 and AS-F1, were anesthetized for nasal and oropharyngeal sample collection on November 8. On November 9, we confirmed SARS-CoV-2 infection in the lions by real-time reverse transcription PCR (rRT-PCR); cycle quantitation (Cq) values were <40. Nasal swab samples from AS-M1 and AS-F1 had the highest viral loads (Cq 23.05 for AS-M1, 24.47 AS-F1). We conducted noninvasive infection monitoring for 3 weeks by collecting

and testing individual and pooled fecal samples from both lion enclosures. AF-M3 had the highest fecal sample viral load, Cq 36.02.

Within 5 days of the index case, 10 lions (all 9 Asiatic and 1 African) were infected. Most (8/10) clinically recovered from respiratory signs within 2 weeks; 2 lions took longer to recover, but all animals had recovered by December 3, 2021. Full recovery in the lions was determined by low viral RNA loads (Cq >40), absence of clinical signs, and resumption of normal behavior.

We sequenced RNA from nasal swab samples of AS-M1 and AS-F1 and 1 fecal sample from AF-M3 on the MinION R9.4.1 (Oxford Nanopore Technology, https://nanoporetech.com) platform using ARCTIC-CoV V1/V3 protocols (J.R. Tyson et al., unpub. data, https://doi.org/10.1101/2020.09.04.283077). The 3GS analysis pipeline from Genome Detective (*3*) generated preliminary contigs, which we stitched together by using sequence alignment information from a zookeeper's publicly available SARS-CoV-2 sequence (GISAID accession no. EPI_ISL_6600690; https://www.gisaid.org). We assessed the assembled sequences by using NextClade (*4*) to identify mutations and frameshifts compared with a wild-type reference sequence (GenBank accession no. NC_045512.2) and subsequently corrected alignment artifacts in the bam file (Appendix 2, https://wwwnc.cdc.gov/EID/article/29/12/22-1916-App2.xlsx).

We assembled 2 complete SARS-CoV-2 genomes (GenBank accession nos. OP393893.1 and OL677176.2) from nasal swab samples collected from AS-M1 and AS-F1. We obtained a partial genome assembly from a fecal sample from AF-M3 but did not analyze it further.

We conducted a phylogenomic analysis on 39 complete viral genomes, comprising 2 genomes from lions in this study and 37 sequences from GISAID, including the zookeeper's sequence. We built a maximum-likelihood tree by using RAxML-ng version 1.1.0 (https://github.com/stamatak/standard-RAxML) with 2,000 bootstrap replicates and used the wild-type reference sequence as the outgroup. The tree revealed that sequences from the zookeeper and Asiatic lions nested within the same subclade (Figure). Those findings and the high (99.98%) viral genetic similarity between the lions and zookeeper strongly suggest that SARS-CoV-2 infection in the

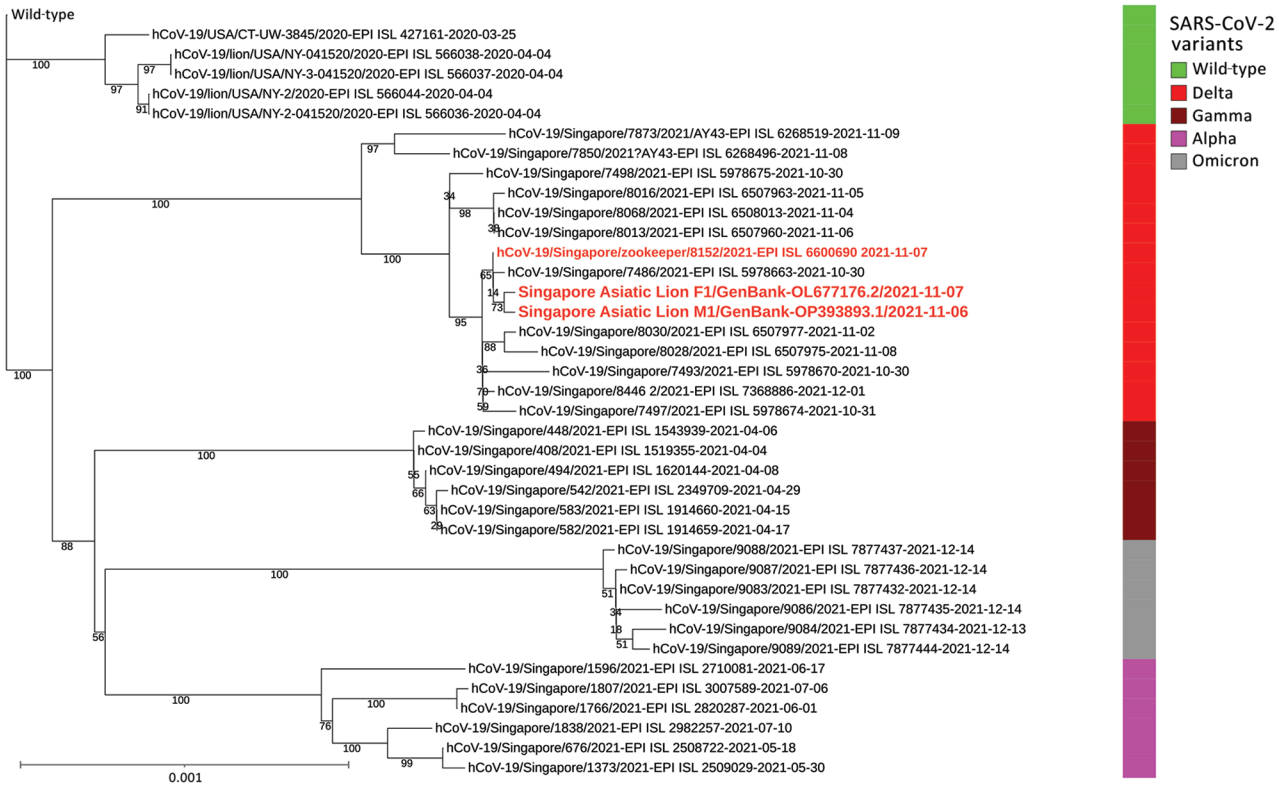

Figure. Maximum-likelihood phylogenomic tree from a case of anthropogenic transmission of SARS-CoV-2 from humans to lions, Singapore, 2021. Tree reconstructed from sequences of 2 lions and 1 zookeeper (red bold text), along with 36 other publicly available sequences representing 4 variants of concern from Singapore, cases of infected lions from the Bronx Zoo, and the wild-type reference genome (GenBank accession no. NC_045512.2) as the outgroup. Scale bar indicates nucleotide substitutions per site. EPI, GISAID (https://www.gisaid.com) EpiFlu database.

lions occurred through a human-to-animal (anthropogenic) transmission route.

We used Pangolin (https://github.com/cov-lineages/pangolin) to identify the subclade as Delta lineage AY.23.1, consistent with the predominant circulating strain in Singapore at that time. Both lions' sequences had 10 key Delta variant spike protein mutations and 2 open reading frame 8 amino acid deletions at positions D119- and F120-, compared with sequences from cases in Singapore (Appendix 1) (*5*). The lions, zookeeper, and 1 community case shared a unique spike protein mutation (S:A1016V), suggesting a potential founder's effect from this anthroponotic transmission event. Our investigation determined that the zookeepers were likely infected 6 days before the lion index case. The lions were not vaccinated against SARS-CoV-2, but 94% of the population of Singapore was fully vaccinated by November 2021.

This study highlights the vulnerability of captive and endangered animal populations to SARS-CoV-2 transmission from humans (*5*–*8*). Close contact between zookeepers and the lions likely led to the transmission, emphasizing the crucial need for strict infection control measures in captive animal facilities, especially during periods of increased community transmission of viruses (*7*).

The implications of SARS-CoV-2 infection in captive lions extend beyond animal health and welfare and can have consequences for the conservation of protected species. Insights from studies on minks and hamsters shed light on the potential for animal-to-human transmission (*6*,*8*). However, mass culling, as noted in those studies of small mammals, is an impractical approach for large or endangered animal species.

Lions already face numerous threats, including habitat loss, poaching, and disease; introduction of a novel virus like SARS-CoV-2 could have devastating consequences for their populations (*7*). Therefore, strengthening biosecurity measures in wildlife conservation centers and promoting vaccination of susceptible animal species whenever feasible and safe are crucial for mitigating viral transmission and protecting vulnerable wildlife populations (*1*,*9*).

Acknowledgments

We thank former and current colleagues of the National Parks Board, Mandai Wildlife Group, for their invaluable assistance and contributions, and the Singapore Immunology Network for supporting the investigation of this incident.

All data are available in the main text or the Appendix materials and can be found on the Zenodo repository at https://doi.org/10.5281/zenodo.8362203. Raw sequence reads generated in this study have been uploaded to the National Center for Biotechnology Information Sequence Read Archive under BioProject no. PRJNA1021696.

The ethical handling of animal subjects during the course of this research has been supervised and approved by National Parks Board, Singapore.

Author contributions: C.L., J.O., and W.K.W. conducted the molecular diagnostic tests; Y.C.A.I. performed the nanopore sequencing for viral genome assembly. Y.C.A.I and A.T. performed data analyses. The figures and the manuscript draft were prepared by Y.C.A.I. with input from C.J.F. Study initiation and guidance was by K.B.H.E, and supervised by C.J.F., S.F.C., Y.H.H., and K.B.H.E. Y.C.A.I. wrote the manuscript and all authors contributed to the manuscript editing process, approved the final version for publication, and declared that the research was conducted in the absence of any commercial or financial relationships that could be construed as a potential conflict of interest.

About the Author

Dr. Ip is a scientific research officer at the Centre for Animal and Veterinary Sciences within the National Parks Board, Singapore. His research interests center around genomic and environmental DNA tools for molecular epidemiology, animal community assessments, rapid detection of pathogens, tracking animal diseases, and studying the dynamics of virus evolution and transmission.

References

1. Mena J, Hidalgo C, Estay-Olea D, Sallaberry-Pincheira N, Bacigalupo A, Rubio AV, et al. Molecular surveillance of potential SARS-CoV-2 reservoir hosts in wildlife rehabilitation centers. Vet Q. 2023;43:1–10. https://doi.org/10.1080/01652176.2023.2164909
2. Tan CCS, Lam SD, Richard D, Owen CJ, Berchtold D, Orengo C, et al. Transmission of SARS-CoV-2 from humans to animals and potential host adaptation. Nat Commun. 2022;13:2988. https://doi.org/10.1038/s41467-022-30698-6
3. Vilsker M, Moosa Y, Nooij S, Fonseca V, Ghysens Y, Dumon K, et al. Genome Detective: an automated system for virus identification from high-throughput sequencing data. Bioinformatics. 2019;35:871–3. https://doi.org/10.1093/bioinformatics/bty695
4. Aksamentov I, Roemer C, Hodcroft EB, Neher RA. Nextclade: clade assignment, mutation calling and quality control for viral genomes. J Open Source Softw. 2021;6:3773. https://doi.org/10.21105/joss.03773
5. Karikalan M, Chander V, Mahajan S, Deol P, Agrawal RK, Nandi S, et al. Natural infection of Delta mutant of SARS-CoV-2 in Asiatic lions of India. Transbound Emerg Dis. 2022;69:3047–55. https://doi.org/10.1111/tbed.14290
6. Kok KH, Wong SC, Chan WM, Wen L, Chu AWH, Ip JD, et al. Co-circulation of two SARS-CoV-2 variant strains

within imported pet hamsters in Hong Kong. Emerg Microbes Infect. 2022;11:689–98. https://doi.org/10.1080/22221751.2022.2040922
7. McAloose D, Laverack M, Wang L, Killian ML, Caserta LC, Yuan F, et al. From people to *Panthera*: natural SARS-CoV-2 infection in tigers and lions at the Bronx Zoo. MBio. 2020;11:e02220-20. https://doi.org/10.1128/mBio.02220-20
8. Oude Munnink BB, Sikkema RS, Nieuwenhuijse DF, Molenaar RJ, Munger E, Molenkamp R, et al. Transmission of SARS-CoV-2 on mink farms between humans and mink and back to humans. Science. 2021;371:172–7. https://doi.org/10.1126/science.abe5901
9. Choudhary OP, Priyanka, Saied AA. COVID-19 vaccination in animals: A strategy for combating the global outbreak. Int J Surg. 2022;105:106848. https://doi.org/10.1016/j.ijsu.2022.106848

Address for correspondence: Yin Cheong Aden Ip, National Parks Board, 6 Perahu Rd, S718827, Singapore 259569; email: aden_ip@nparks.gov.sg

Mass Mortality of Sea Lions Caused by Highly Pathogenic Avian Influenza A(H5N1) Virus

Víctor Gamarra-Toledo,[1] Pablo I. Plaza,[1] Roberto Gutiérrez, Giancarlo Inga-Diaz, Patricia Saravia-Guevara, Oliver Pereyra-Meza, Elver Coronado-Flores, Antonio Calderón-Cerrón, Gonzalo Quiroz-Jiménez, Paola Martinez, Deyvis Huamán-Mendoza, José C. Nieto-Navarrete, Sandra Ventura, Sergio A. Lambertucci

Author affiliations: Grupo de Investigaciones en Biología de la Conservación, Laboratorio Ecotono, INIBIOMA, Universidad Nacional del Comahue—CONICET, Bariloche, Argentina (V. Gamarra-Toledo, P.I. Plaza, S.A. Lambertucci); Museo de Historia Natural, Universidad Nacional de San Agustín de Arequipa, Arequipa, Peru (V. Gamarra-Toledo, R. Gutiérrez); Servicio Nacional de Áreas Naturales Protegidas por el Estado, Lima, Peru (R. Gutiérrez, G. Inga-Diaz, P. Saravia-Guevara, O. Pereyra-Meza, E. Coronado-Flores, A. Calderón-Cerrón, G. Quiroz-Jiménez, P. Martinez, D. Huamán-Mendoza, J.C. Nieto-Navarrete, S. Ventura); Asociación Convive Perú, Madre de Dios, Perú (G. Inga-Diaz)

DOI: http://doi.org/10.3201/eid2911.230192

[1]These two authors contributed equally to the study.

We report a massive mortality of 5,224 sea lions (*Otaria flavescens*) in Peru that seemed to be associated with highly pathogenic avian influenza A(H5N1) virus infection. The transmission pathway may have been through the close contact of sea lions with infected wild birds. We recommend evaluating potential virus transmission among sea lions.

The panzootic (2020–2023) caused by the highly pathogenic avian influenza (HPAI) A(H5N1) caused numerous global outbreaks in 2022 (*1*). At the end of the year, the H5N1 virus reached South America, causing alarming bird mortalities in Peru (*2*). Comprehensive surveys suggest the virus killed >100,000 wild birds by the end of March 2023 only in protected areas (and >200,000 birds including other areas); particularly affected were Peruvian boobies (*Sula variegata*), guanay cormorants (*Leucocarbo bougainvilliorum*), and Peruvian pelicans (*Pelecanus thagus*) (*3*). The large biomass of infected wild birds may have led to a spillover event affecting marine mammals cohabiting with them, as reported in other parts of the world (*4*). Here, we report the death of several thousand sea lions (*Otaria flavescens*) on the coast of Peru within a few months; the sea lions manifested neurologic and respiratory signs. Clinical signs we observed suggest they were affected by HPAI H5N1, which was later confirmed by government and scientific reports (*5*,*6*).

During January–April 2023, we performed detailed surveillance of dead and agonal sea lions in protected marine areas of Peru (Figure). We found 5,224 animals dead or dying on beaches (Table). The synchronized high mortality rate we observed was concerning; up to 100 dead animals were found floating together in the sea, and 1,112 animals died on 1 island that has one of highest populations of sea lions in Peru (San Gallan, Ica, Reserva Nacional Paracas; Table). Those unprecedented massive mortalities for this region and even the entire world killed ≈5% of Peru's population of this species in a few months (Figure, panels A, B; Appendix Figure, https://wwwnc.cdc.gov/EID/article/29/12/23-0192-App1.pdf) (*7*).

National health authorities implemented restrictions regarding the manipulation of sick animals; for this reason, we were able to perform 1 necropsy, and the other observations were made by veterinarians at prudent distance. The clinical signs of agonal individuals were mainly neurologic, such as tremors, convulsions, and paralysis URLs (Video 1, https://wwwnc.cdc.gov/EID/article/29/12/23-0192-vid1; Video 2, https://wwwnc.cdc.gov/EID/

Article DOI: https://doi.org/10.3201/eid2912.221916

EID cannot ensure accessibility for supplementary materials supplied by authors. Readers who have difficulty accessing supplementary content should contact the authors for assistance.

Anthropogenic Transmission of SARS-CoV-2 from Humans to Lions, Singapore, 2021

Appendix 1

Wet Laboratory and Phylogenomic Analyses Methods

Viral RNA Extraction and RT-qPCR Amplification

The swab samples were placed in virus transport media while blood samples were added to tubes with ethylenediaminetetraacetic acid (EDTA) and transported on ice to CAVS for laboratory diagnostic investigation. Upon receipt of samples, nasal and oropharyngeal swabs were vortexed for 15 s and placed in 1.5 mL eppendorf tubes for ribonucleic acid (RNA) extraction. Fecal samples were diluted 1:10 in virus transport media (VTM), vortexed for 15 s, pulse centrifuged and the decant was used for RNA extractions. EDTA blood samples were processed directly. Viral RNA was extracted using QIAGEN IndiMag Pathogen Kit on an automated nucleic acid extraction machine Applied Biosystems MagMax Total Nucleic Acid Extraction System using manufacturer's protocols and eluted in 100 µL of elution buffer.

Preliminary detection of SARS-CoV-2 from RNA extracts was ascertained with three assays, (i) screening (E assay for betacoronavirus), (ii) confirmatory (C assay for SARSCoV) and (iii) discriminatory (D assay for SARS-CoV-2) with real-time reverse transcription polymerase chain reaction assays (rRT-PCR) on the Applied Biosystems 7900 Fast. All three rRT-PCR assays were done in a total volume of 25 µL reaction mixture, consisting of 12.5µL of 2′ RT-PCR buffer (Applied Biosystems AgPath-ID One Step RT-PCR reagents), 1µL of 25′ RT-PCR enzyme mix, 2.5 µL of RNA template, with varying volumes in primers and probes: (i) E assay: 1 µL (10 µmol) each of forward: E-Sarbeco-F1 ACAGGTACGTTAATAGTTAATAGCGT and reverse: E-Sarbeco-R2 ATATTGCAGCAGTACGCACACA primers, 1 µL (6 µmol) of probe: E-Sarbeco-P1

FAMACACTAGCCATCCTTACTGCGCTTCGBBQ, and 6 µL of nuclease-free water; (ii, iii) D and C assays: 1.5 µL (10 µmol) of forward: RdRp-SARSr-F2 GTGARATGGTCATGTGTGGCGG and 2 µL of reverse: RdRp-SARS-R1 CARATGTTAAASACACTATTAGCATA, 1 µL (6 µmol) of probe: RdRp-SARSr-P2 FAM-CAGGTGGAACCTCATCAGGAGATGCBBQ, and additional probe RdRp-SARSr-P1 FAM-CCAGGTGGWACRTCATCMGGTGATGCBBQ for C assay, and finally 4.5 µL and 3.5 µL of water for D and C assays respectively. The thermal cycling profile consisted of an initial reverse transcription step at 45°C for 10 minutes, an initial enzyme activation step at 95°C for 10 minutes, followed by 45 cycles of 94°C for 15 seconds and 58°C for 30 seconds. Samples that returned a Cq value of <42 were considered as a detection of SARSCoV-2 nucleic acid material.

Multiplex PCR and Oxford Nanopore Sequencing and Assembly of SARS-CoV-2 Genomes

Two RNA samples from nasal swabs of two Asiatic lions (Cq = 23.05 and 24.47) and one individual fecal sample from an African lion (Cq = 36.02) were sequenced on the MinION Nanopore platform. One of the nasal swab samples (viral inactivated at 56 degrees for 2 hours) was re-extracted using QIAamp Viral RNA extraction kit following manufacturer's instructions. All post-PCR, reverse transcription, and library purification steps were done with KAPA pure beads (Roche Sequencing).

Nasal swab RNA was converted directly to double-stranded complementary DNA (cDNA) by first-strand synthesis with the SuperScript III kit (Thermo Fisher Scientific) containing random hexamers. Briefly, 1 µL each of dNTPs and random hexamers (50 µmol, Invitrogen) were added to 11 µL of template RNA and incubated at 65°C for 5 minutes before placing on ice for 1 minute. Next, 1 µL of 0.1M DTT, 4 µL of 5′ First Strand buffer, 1 µL of RNaseOUT (Invitrogen) and 1 µL of SuperScript III were added to each cDNA conversion reaction assay of the previous step. The final 20 µL mix was incubated at 42°C for 50 minutes, followed by 70°C for 10 minutes, and placed on ice for 5 minutes. The PCR reaction products were purified, and cDNA was stored at −20°C until library preparation.

Separately, the single fecal sample underwent a Sequence-Independent Single Primer (SISPA) enrichment (*1*) to increase nucleic acid yield for whole genome sequencing (*2*,*3*). Briefly, first-strand cDNA was synthesized in a 20 µL reaction consisting of 7 µL of viral RNA

from fecal samples, 50 pmol of 10 µmol primer A (5′- GTTTCCCACTGGAGGATA-NNNNNNNNN- 3′), SuperScript III

Reverse transcription (Thermo Fisher Scientific) and dNTPs (10 µmol), with incubation at 25°C for 5 minutes, followed by 50°C for 60 minutes and 70°C for 15 minutes. Second strand synthesis continued in the 20 µL cDNA mix forming a total volume of 24 µL with 2.5 µL Klenow buffer, 10 pmol Primer A, and dNTPs (1 µmol), with one-hour incubation at 37°C. The doublestranded cDNA was purified, and sequence-independent PCR amplification was done in a final reaction volume of 50 µL containing 2× LongAmp® Taq Master Mix (NEB), 50 pmol of 10 µmol primer B (5′- GTTTCCCACTGGAGGATA-3′). The PCR cycling was performed as follows: 94°C for 30 s, followed by 30 cycles of 94°C for 15 s, 50°C for 30 s and 65°C for 5 minutes, with a final extension at 65°C for 10 minutes, followed by purification of PCR products.

Multiplex PCR was used to enrich viral cDNA of all three samples using Q5 Hot-start HF polymerase with ARCTIC-CoV V1 and V3 protocols (J.R. Tyson et al., unpub. data, https://doi.org/10.1101/2020.09.04.283077), where the tiling primer schemes targeted SARS-CoV-2 genome-wide amplicons of 400-bp in length. PCR thermal cycling profiles consisted of 98°C at 30 seconds, followed by 25 (Cq <25 nasal swab samples) or 35 cycles (Cq: 36.02 fecal samples) of 98°C for 15 seconds and 65°C for 5 minutes, before a final placement on ice for 5 minutes. Forward and reverse primer PCR reactions (odd and even primer pools) were conducted separately and pooled immediately after PCR, purified, and end-repaired with the NEB Ultra II companion kit.

MinION nanopore libraries were prepared using the Native Barcoding (EXP-NBD104) and ligation sequencing (SQK-LSK109) kits (Oxford Nanopore Technologies, Oxford, UK). Finalized cDNA libraries of 8–12 ng were loaded on three Flo-MIN106 R9.4 flow cells and sequenced for 22–36 hours.

Phylogenomic Analyses

MAFFT v. 7.490 to generate multiple sequence alignments for the 39 sequences intended for tree inference (Figure in main article text). The final alignment only consisted of coding regions and stop codons were verified to be present only at the terminal end of each gene. Next, RaxML-ng v1.1.0 was used to infer a maximum-likelihood tree, using the GTR + I + G model of

nucleotide substitution with 2000 bootstrap replicates, and the Wuhan-Hu-1 reference sequence (GenBank: NC_045512.2 / GISAID: EPI_ISL_402119) was used as the outgroup. Convergence of trees were attained at 1950 bootstraps. Inferred trees were visualized and annotated on Interactive Tree of Life v5 (iTOL) (*4*).

Bioinformatic Analyses

Genome Detective Assembly of Nanopore Reads.

Consensus sequences were generated by Genome Detective using a consensus algorithm that is reference based for 3GS reads (J.R. Tyson et al., unpub. data, https://doi.org/10.1101/2020.09.04.283077). For nasal swab samples from AS-M1 and AS-F1, the consensus viral sequences consisted of 29,822 bp, had mean read depths of 364.99 and 1,050.59, median read depths of 199 and 466, read depth ranges of 2–3,013 and 1–11,918, and mean base quality scores of 19.1 and 19.3.

Long reads are blasted to candidate reference sequences (NT&AA), aligned with aga (a combined NT&AA aligner, https://www.genomedetective.com/app/aga) to the top candidates, the consensus sequences are then constructed. Due to aligning in the NT and AA domain simultaneously, aga is able to detect and correctly handle frame shifts, and also corrects errors in monomer repeat regions as those errors are typical for nanopore sequencers.

Stitching of Sequences

The consensus contigs obtained from Genome Detective were aligned to the Singapore reference SARS-CoV2 sequence (EPI_ISL_6600690). Based on this reference, the gaps were determined. Passed nanopore reads (Q-score $\geq$8) were mapped using Minimap2 to this reference and the consensus bases (Base Quality $\geq$10) in the reads that encompassed these gaps were used to stitch the contigs together. The consensus cut off was at 80%, but when the cut off cannot be achieved, an N base was used as a fill in. No explicit depth cut off filter was applied in this analysis. Instead, the depth filter is implicitly defined with a consensus 80% cut off as demonstrated in Appendix 1 Table 1.

Appendix 1 Table 1. Relationship between depth and consensus for SARS-CoV-2 sequences

Depth	Minimum consensus bases	% Effective consensus
1	1	100
2	2	100
3	3	100
4	4	100
5	4	80
6	5	83
7	6	86
≥6	...	...

Thus, the consensus cut off is more stringent for lower depths as seen in the table. Insertions and deletions were not encountered during the stitching process.

The rationale for this approach is that our sequencing runs included sequence fragments that were not reliably amplified by the ARCTIC V1 and V3 primers. These regions would have low read depth and thus were filtered out during the consensus building process.

0.51% and 2.4% of the nucleotides for AS-F1 and AS-M1 sequences were added during this process. Note that for a portion of AS-F1, the read depths were high but that region was not included in the consensus sequence generated by Genome Detective (Appendix 1 Table 2). The script for stitching is available at https://github.com/atks/cavs/blob/master/var/analysis/stitch_contigs.py.

Appendix 1 Table 2. Consensus sequences generated by Genome Detective*

Sequence	Length, bp	No. contigs to stitch	Added sequences (N bases)	Mean depth	Gap depths	Gap added bases
AS-F1	29825	2	153 (2Ns)	451.14	1475.96, 8.00, 15.05	46, 68, 39
AS-M1	29861	4	706 (30Ns)	11.7	1.77, 6.66, 7.75, 22.3, 9.55	13, 252, 179, 213, 49

*bp, base pairs.

Manual Polishing of AS-F1 Stitched Sequence

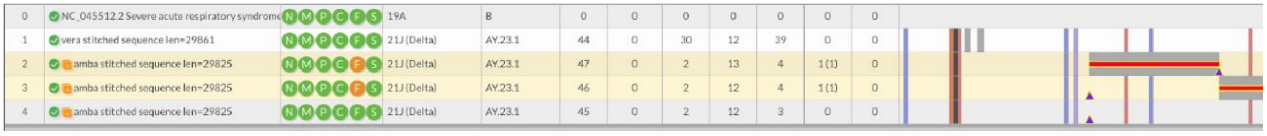

Appendix 1 Figure 1. NextClade Output showing mutations in this stud's viral genomes when compared with the reference genome.

The mutations detected by NextClade (Appendix 1 Figure 1) were examined in the mapped reads to remove any artifacts introduced by Genome Detective. These changes are summarized in Appendix 1 Figures 2–5.

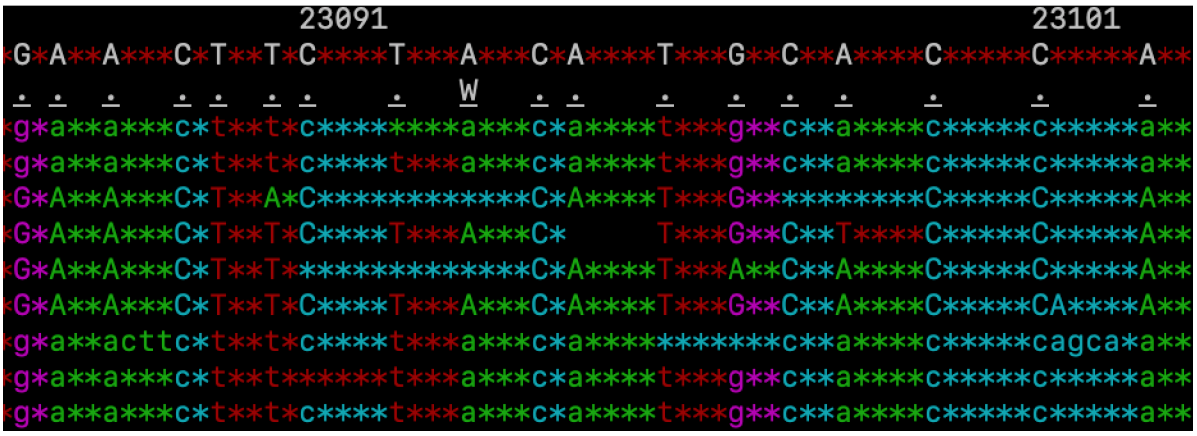

Appendix 1 Figure 2. Position 23093–23095 consisting of 2 populations of haplotypes – ACAT and TCAT. The sequence from Genome Detective has TAC in place that induces a frameshift. Changing TAC >ACAT removes the frameshift but introduces an inserted Proline CCT and a downstream frameshift.

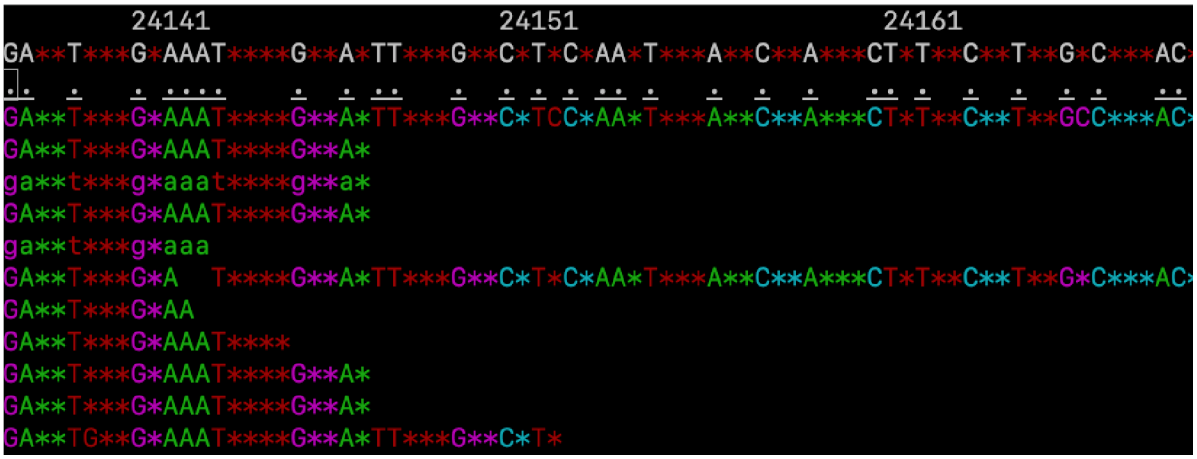

Appendix 1 Figure 3. Position 24151–24154. The sequence from Genome Detective has GGTG, this is detected at a position where Minimap2 soft clips many reads. There are nonetheless reads that give support to show that the reference sequences are largely conserved. Position 23093 has two populations of reads with A and T bases. We replaced GGTG with TTG due to the reads supporting the reference. Frameshift has been removed.

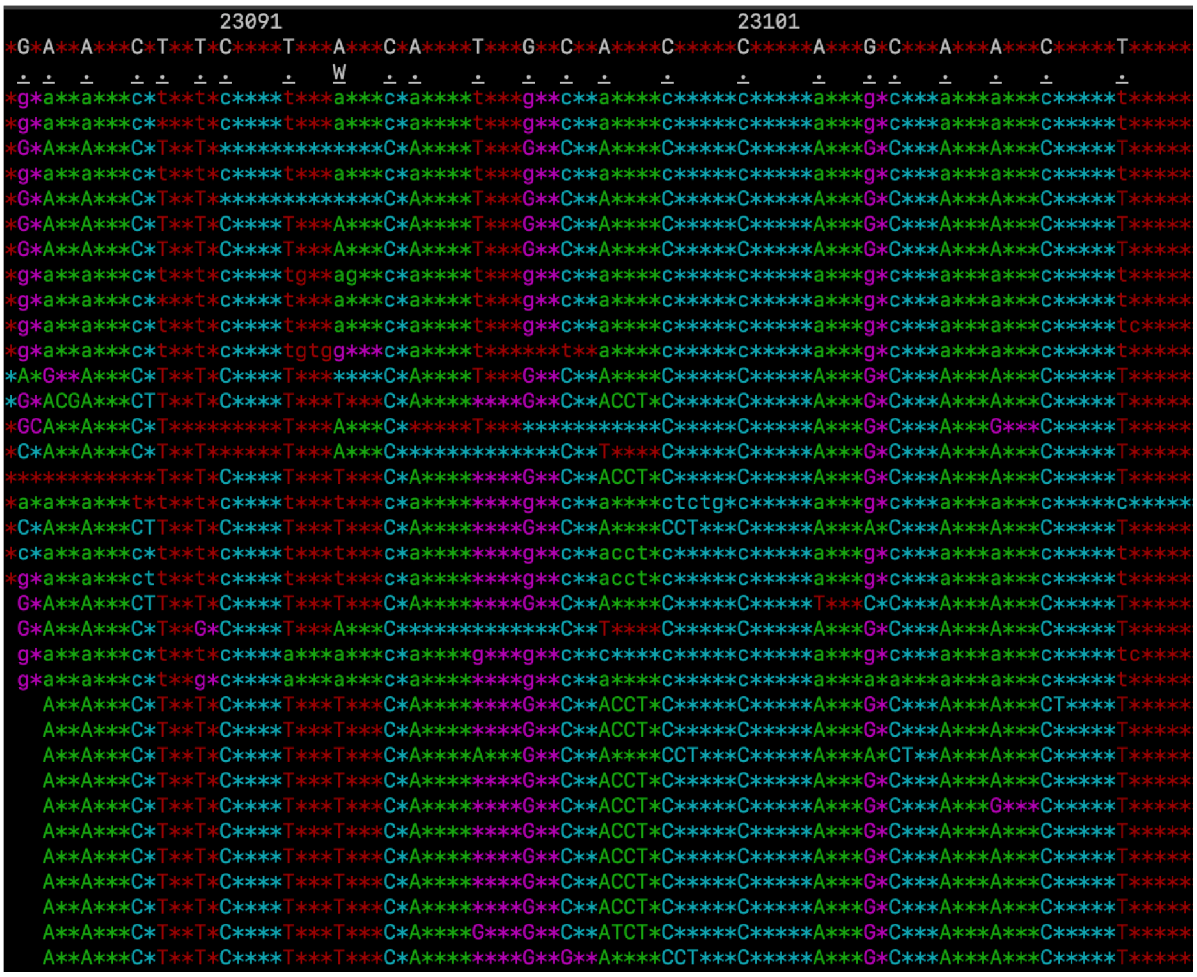

Appendix 1 Figure 4. Positions 23100–23102 contain the inserted CCT proline codon. Once again, there are two populations of reads. However, the CCT sequence tends to occur on the tail end of reads and accompanies the T base variant at position 23093. We defer again to the reads that support the reference sequence. CCT has been deleted.

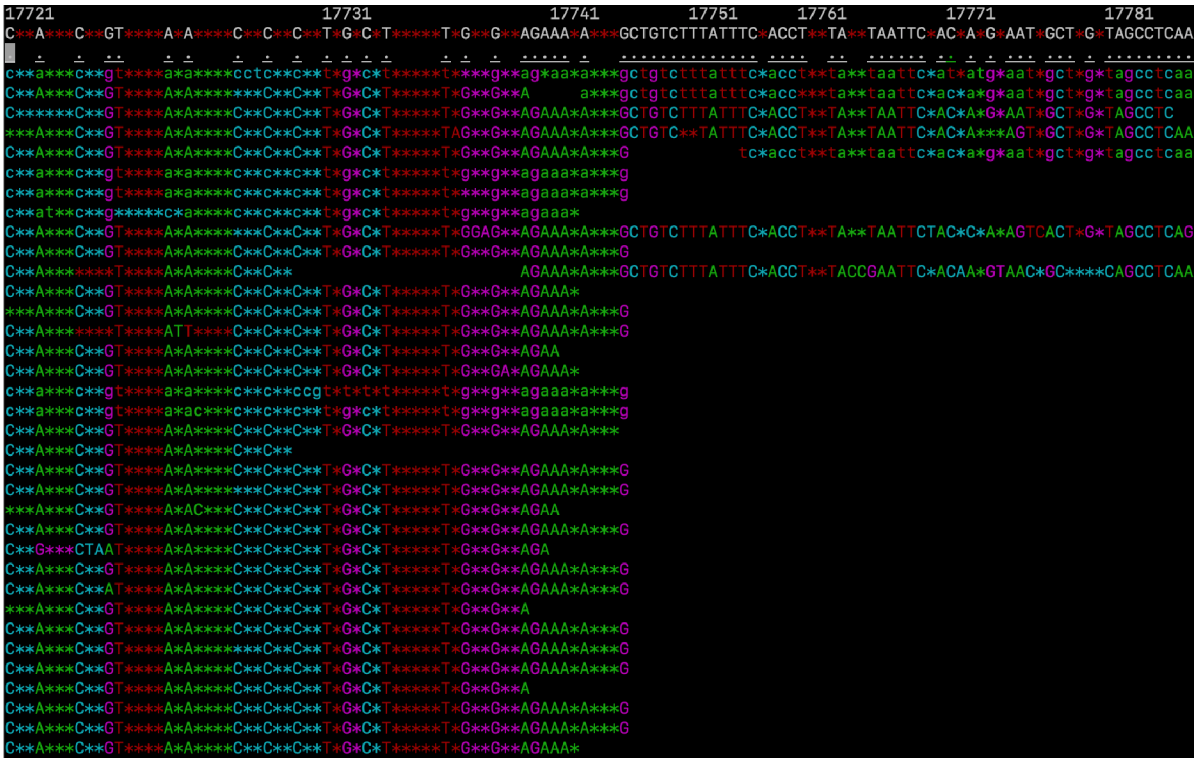

Appendix 1 Figure 5. Position 17762 is reported to be an A missense mutation in Genome Detective's sequence. The allele, however, occurs on the soft clipped portion of many Minimap2 reads. There are reads that support the reference, thus we changed the base from A to C.

Manual Polishing of AS-M1 Stitched Sequence

The mutations detected by NextClade were examined in the mapped reads to remove any artifacts introduced by Genome Detective. These changes are summarized in Appendix 1 Figure 6.

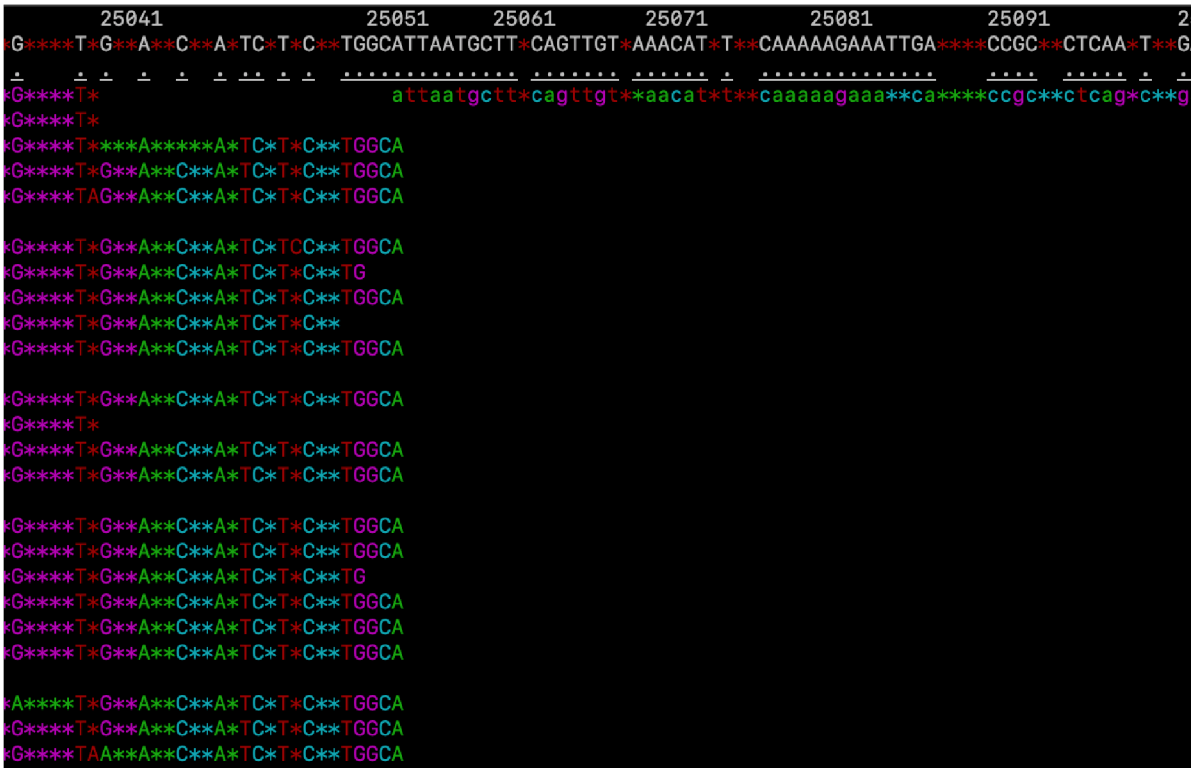

Appendix 1 Figure 6. Position 25054–25092. Large 13 AA insert appears to be soft clipped on Minimap2 alignments. AGGTGCTGCAGGTAGAAAGAAGCAGAATCGGATTAACCC = >delete.

Coverage of Arctic V1 and V3 Primers

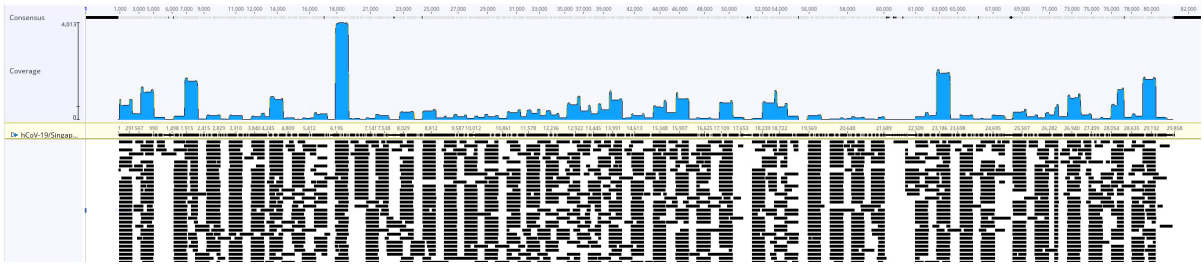

Appendix 1 Figure 7. Coverage of Arctic V1 and V3 primers for samples from Asiatic lion AS-F1.

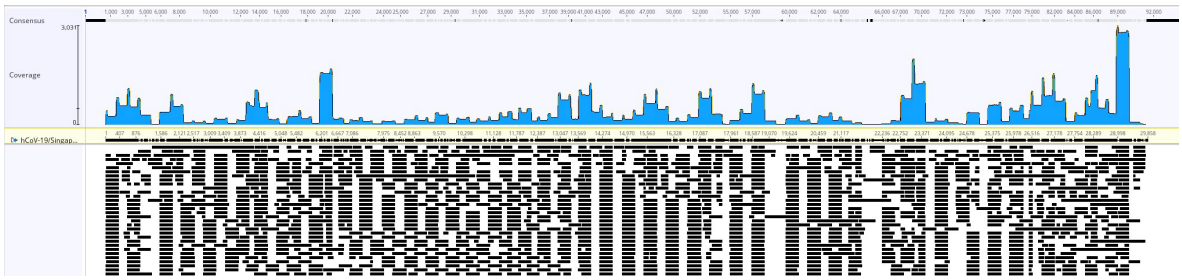

Appendix 1 Figure 8. Coverage of Arctic V1 and V3 primers for samples from Asiatic lion AS-M1.

References

1. Chrzastek K, Lee DH, Smith D, Sharma P, Suarez DL, Pantin-Jackwood M, et al. Use of sequence-independent, single-primer-amplification (SISPA) for rapid detection, identification, and characterization of avian RNA viruses. Virology. 2017;509:159–66. PubMed https://doi.org/10.1016/j.virol.2017.06.019

2. Fernández-Bellon H, Rodon J, Fernández-Bastit L, Almagro V, Padilla-Solé P, Lorca-Oró C, et al. Monitoring natural SARS-CoV-2 infection in lions (*Panthera leo*) at the Barcelona Zoo: viral dynamics and host responses. Viruses. 2021;13:1683. PubMed https://doi.org/10.3390/v13091683

3. Mishra A, Kumar N, Bhatia S, Aasdev A, Kanniappan S, Sekhar AT, et al. SARS-CoV-2 Delta variant among Asiatic lions, India. Emerg Infect Dis. 2021;27:2723–5. PubMed https://doi.org/10.3201/eid2710.211500

4. Letunic I, Bork P. Interactive Tree Of Life (iTOL) v5: an online tool for phylogenetic tree display and annotation. Nucleic Acids Res. 2021;49:W293–96. PubMed https://doi.org/10.1093/nar/gkab301

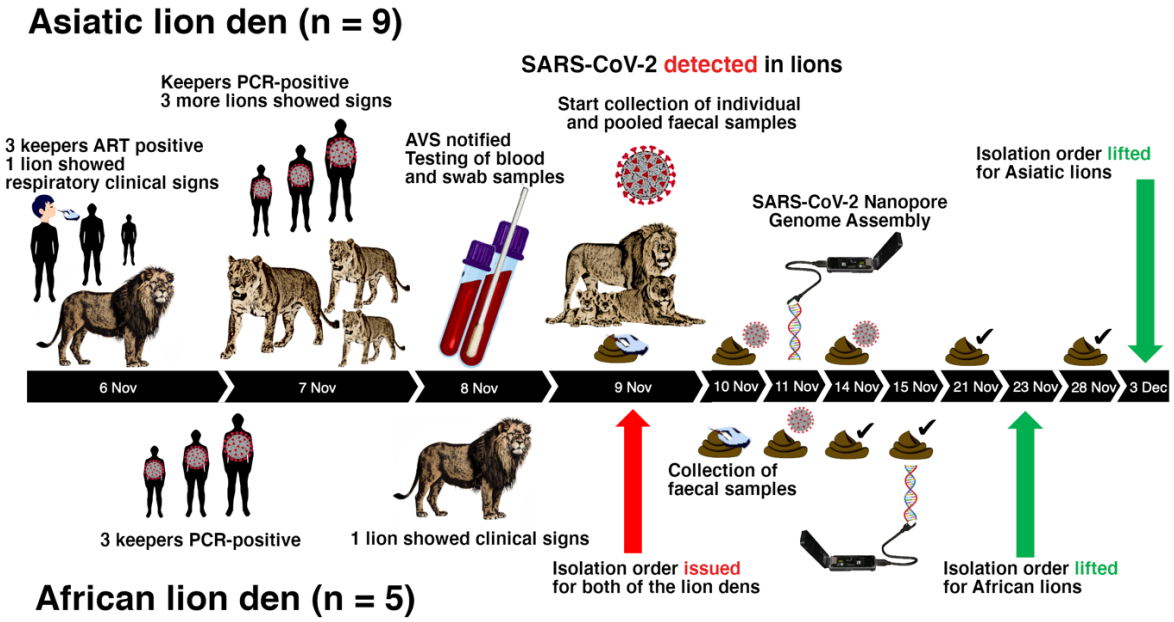

Appendix 1 Figure 9. Timeline of events providing an overall graphical summary of SARS-CoV-2 infections of lions and zookeepers at the MWG, and the subsequent diagnostic efforts by CAVS for confirmation and surveillance of infection up till recovery.

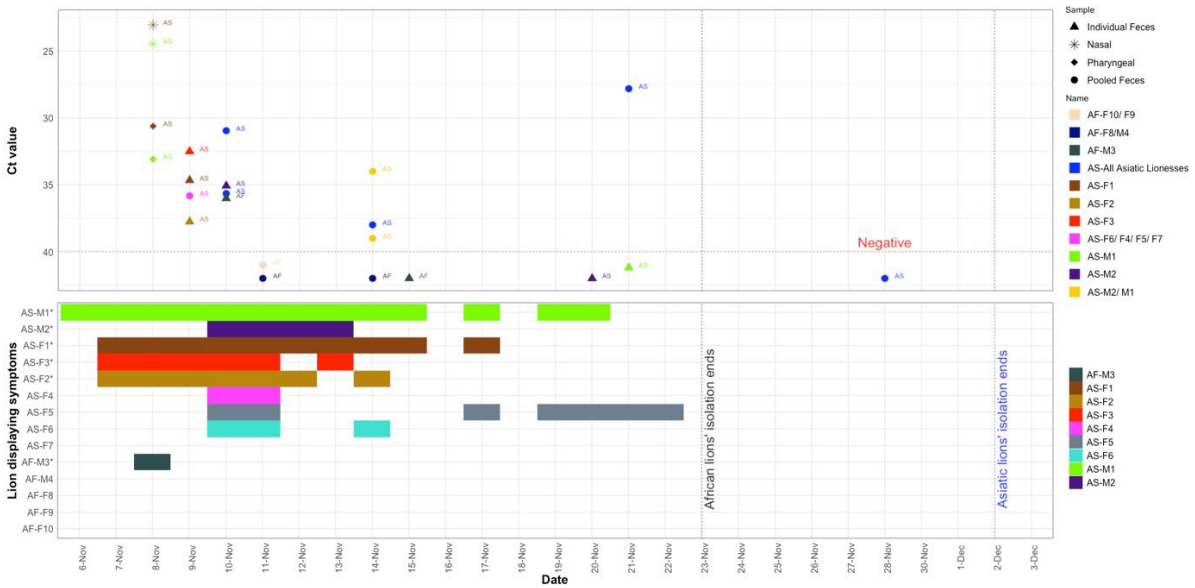

Appendix 1 Figure 10. Tracking viral RNA detection trends of all naturally infected lions (colors) using rRT-PCR on nasal swab, oropharyngeal swab, and fecal samples; represented by symbols (upper panel) and are largely congruent with the recorded clinical observations of signs (lower panel). African and Asiatic lions are indicated by codes "AF" and "AS" in the legends and data points, respectively.

Appendix 1 Figure 11 (following page). Maximum likelihood tree inferred from Singapore's community cases during October 25–November 23, 2021. The tree consists of 1,003 genomes that include the wildtype as outgroup, zookeeper sequence, and M1 and F1 sequences from lion cases.